DOI: https://doi.org/10.68732/d54c80b62e28d88b

ISBN: 978-9989-2053-6-1

Replica-based experimental framework for characterizing fluid flow in a dislocated fracture

S. L. Vidanage, M. Torkan, M. Janiszewski, M. Rinne & L. Uotinen
Department of Civil Engineering, School of Engineering, Aalto University, Espoo, Finland
sandaru.liyanarathnavidanage@aalto.fi
0009-0002-2790-0589

Abstract

Fractures significantly impact fluid flow in rock masses and comprehending how dislocations influence fracture-controlled flow is important for evaluating fluid movement in geological engineering applications, particularly for the long-term safety of geological nuclear waste disposal sites.

In this method, A 6 cm × 6 cm × 10 cm Kuru granite specimen containing an induced tensile fracture was scanned using photogrammetry. Photogrammetry was used to capture the fracture surfaces and aperture geometries of the perfectly matched state and each dislocation step of the specimen's upper half, using markers with known distances to accurately align and scale the dislocated surfaces.

The 3D models of the upper and lower surfaces of the physical aperture were then modelled for each dislocation step and reproduced using Fused Deposition Modelling (FDM) 3D printing. The printed aperture models incorporated an inlet and outlet to allow fluid flow testing within a fully watertight assembly, enabling precise measurements through accurately replicated apertures. This configuration provided controlled experimental conditions and enhanced the reliability and precision of the flow data. A custom fluid-flow apparatus was developed to measure flow rates through the replicas at varying water pressures, enabling experimental examination of the effects of dislocation on fluid-flow behaviour. Further results were evaluated through the Forchheimer equation for hydraulic aperture calculation.

The fluid flow tests revealed that increasing fracture dislocation results in higher flow rates, following a nonlinear relationship with the pressure gradient and leads to increased hydraulic apertures up to the tested limit of 5 mm dislocation. However, limitations related to the replication of fracture surfaces and physical apertures in 3D printing and photogrammetry must be assessed to ensure the accuracy of the results.

Keywords

Fracture, Dislocation, Fluid flow, Photogrammetry, 3D printing.

1 Introduction

Fractures play a key role in determining the mechanical strength and fluid flow characteristics of rock masses. The behaviour of fluid flow through fractures can be studied either at the scale of single fractures or across a rock mass with many interconnected fractures. Ultimately, the overall conductivity of a rock mass depends on how well the fractures are connected and on the hydraulic properties of each fracture (Hakami 1995). A thorough understanding of single-fracture behaviour is necessary before interpreting the behaviour of fractured rock masses (Hakami and Larsson 1996).Darcy's law, which assumes linear flow, often fails to accurately capture flow behaviour in rock fractures with rough and non-parallel surfaces. This is because natural fractures exhibit complexities such as surface roughness, matedness, variations in physical aperture, and contact areas. These factors lead to deviations from Darcy flow, resulting in nonlinear flow behaviour (Zimmerman et al. 2004).

The Forchheimer lawis widely used to describe the fluid flow through porous media, and it is generally accepted to explain the nonlinear fluid flow behaviour through roughed rock fractures (Zimmerman et al. 2004). Therefore, nonlinear fluid flow through a rock fracture with rough and non-parallel surfaces can be described using the adaptation of Forchheimer's equation (Eq. 1) and is characterised by the term hydraulic aperture (e_h), which is defined as the equivalent aperture between two smooth parallel flat plates that would permit the same flow rate with laminar flow, assuming that the flow follows Darcy's law under an identical pressure gradient.

$$-\nabla P = \left(\frac{12\mu}{we_h^3}\right) Q + \left(\frac{\beta\rho}{w^2 e_h^2}\right) Q^2 \#(1)$$

$$-\nabla P = \frac{\Delta P}{L} \#(2)$$

Here, Q denotes the flow rate (m^3/s), and ∇P is the pressure gradient (Pa/m). The hydraulic aperture is given by e_h (m), while μ is the dynamic viscosity of water (8.90×10^{-4} Pa·s), and w is the fracture width (m). The density of water is represented by ρ (997 kg/m^3), and β denotes the non-Darcy coefficient (1/m). The pressure drop across the fracture length L (m) in the direction of flow is expressed as ΔP.

However, investigating fluid flow using natural rock specimens presents several challenges, especially when fractures have dislocations and complex geometries that are difficult to replicate with precision. Experimental studies are further constrained by specimen size, limitations in testing equipment, and difficulties in controlling fracture geometry. In addition, achieving identical experimental conditions is challenging, which reduces the repeatability of results. To overcome these issues, a method integrating high-resolution photogrammetry, 3D modelling, and 3D printing has been developed in this study. This approach enables the production of accurate fracture replicas with controlled dislocations, allowing fluid flow to be studied under both aligned and dislocated fracture conditions.

Photogrammetry is widely applied to characterise rock fracture geometries and evaluate their hydro-mechanical behaviour (Uotinen et al. 2020). It provides a means to reconstruct individual fracture surfaces in detail, enabling assessment of surface roughness and physical aperture. In addition, this approach has been developed to reconstruct both halves of a fractured rock specimen within a unified coordinate system, ensuring accurate spatial alignment (Torkan et al. 2024). Among 3D printing methods, Fused Deposition Modelling (FDM) is widely used to replicate the joint and fracture features of rock masses with high geometric accuracy. 3D printing in rock mechanics enables controlled and repeatable experiments by producing uniform rock replicas while preserving the original specimens. It also enables the creation of complex geometries, reducing the variability found in natural samples for more controlled experimental studies (Jiang and Zhao 2015).

2 Methodology

2.1 Preparation of the specimen and photogrammetry

A Kuru granite specimen measuring 6 cm × 6 cm × 10 cm was divided into upper and lower halves using the plug-and-feather technique to produce a tensile fracture. The different sides of the specimen, as well as the upper and lower fracture surfaces, were marked with lines for identification. The number of lines indicates the respective side number, ranging from 1 to 4(Fig. 1).



(a) (b) (c)

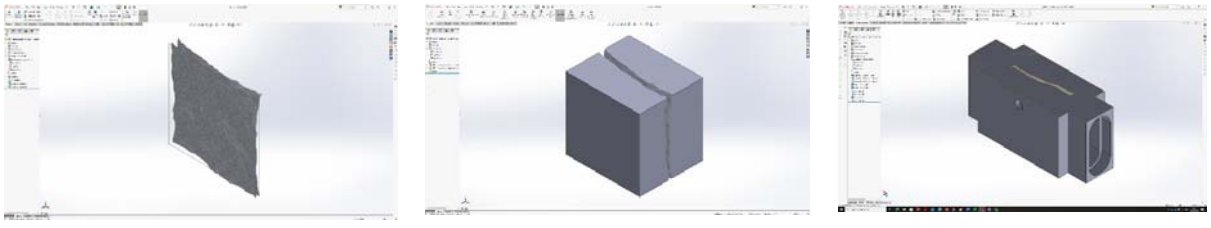
Fig. 1 The Kuru granite specimen with dimensions of 6 cm × 6 cm × 10 cm: (a) in perfectly matched position, (b) the lower half, and (c) the upper half (Torkan *et al.*, 2025).

Photogrammetry was used to generate high-resolution 3D models of the fractured surfaces in both perfectly matched (non-dislocated) and dislocated states. For the dislocated cases, the upper half of the specimen was shifted in the ±X and ±Y directions by 1, 2, 3, 4, and 5 mm (Fig. 4b-c). These displacements were measured using a calliper with a 10 µm resolution. A series of overlapping images was processed in RealityCapture software to produce scaled and properly oriented 3D point clouds for both the matched and dislocated configurations. The accuracy of the models was assessed using root mean square error (RMSE) analysis based on known distances between predefined markers and ceramic calibration blocks of fixed dimensions placed around the specimen. The accuracy assessment yielded RMSEs of 36µm for scale bars and 16-60 µm for ceramic blocks. The detailed description of the photogrammetry workflow, 3D reconstruction process, and accuracy evaluation is provided in a previous study, where the physical aperture of the dislocated fracture in the same specimen was also determined using the same high-resolution photogrammetric method (Torkan et al. 2025).

2.2 3D Modelling of physical aperture of non- and dislocated fracture

After reconstruction and texturing in RealityCapture, the 3D point clouds of the upper and lower halves were exported in *.xyz format and then imported into CloudCompare software. Within CloudCompare, the rough fracture surfaces of each half were trimmed to remove non-essential regions. These cropped surfaces were subsequently used to reconstruct both the dislocated and perfectly matched fracture models in a common coordinate system. For 3D printing of rough surfaces with physical aperture, the point clouds of the upper and lower specimen surfaces, both individually and combined, were meshed using CloudCompare. The resulting surface meshes were then exported in *.ply format for further processing in SOLIDWORKS software.

In SOLIDWORKS, the upper and lower surfaces of the aperture were created as two separate components. First, the imported upper or lower surface of the physical aperture was scaled and re-meshed within the software (Fig. 2a). The mid-surface of the mesh was then used as the reference plane, and the geometry was symmetrically extruded in both directions to form a solid body. After extrusion, the “Cut with Surface” feature was applied to emboss the fracture surface while obtaining the respective halves in the accurate orientation (Fig. 2b). The resulting halves were then assembled, maintaining a 0.4 mm separation between the upper and lower surfaces (Fig. 2c). This spacing was introduced to avoid underestimation of the physical aperture caused by potential nozzle interference during the 3D printing process (Fig. 7a).



(a) (b) (c)

Fig. 2 Modelling of the physical aperture: (a) Imported fracture surfaces after scaling and remeshing; (b) Assembly of the reconstructed upper and lower fracture surfaces; (c) Final assembly of the fracture model, including connector openings.

2.3 3D Printing of physical aperture of non- and dislocated fracture

Each 3D-printed physical aperture model, representing either a perfectly matched or dislocated specimen, was fitted with inlet and outlet connectors for the intended flow direction of the experiment (Fig. 3a). This design was developed to ensure a fully watertight test assembly, enabling accurate fluid flow measurements through a precisely replicated physical aperture of both perfectly matched and dislocated fractures. The aim was to obtain more reliable data under controlled conditions in a simpler

and more accurate testing procedure. The final model, including the connectors, was then exported for 3D printing in *.3mf format using the "Print 3D" function with high-quality settings, ensuring a fully watertight printable object.

Ultimaker Cura 5.7.2 was used as the slicing software for 3D printing, with customised parameters as listed in Table 1. The model was oriented so that one side of the aperture surface was placed directly on the build plate. The printing was performed using an Ultimaker 3 Extended Fused Deposition Modelling (FDM) printer equipped with an AA 0.25 mm nozzle. Polyethylene terephthalate glycol-modified (PET-G) was used as the printing material.

Table 1. 3D printing parameters and settings used.

Parameter	Value	Notes
Layer height	0.050 mm	Quality
Line width	0.25-0.26 mm	Quality
Print speed	55 mm/s	For PET-G
Nozzle temperature	235 ℃	For PET-G
Build plate temperature	85 ℃	For PET-G
Build plate temperature initial layer	90 ℃	For PET-G
Z seam alignment	Random	Walls
Build plate adhesion type	None	-
Remove all holes	Enable	Mesh fixes
Maximum resolution	0.02 mm	Mesh fixes
Enable fluid motion	disable	Mesh fixes
Slicing tolerance	Middle	Experimental

2.4 Fluid flow test

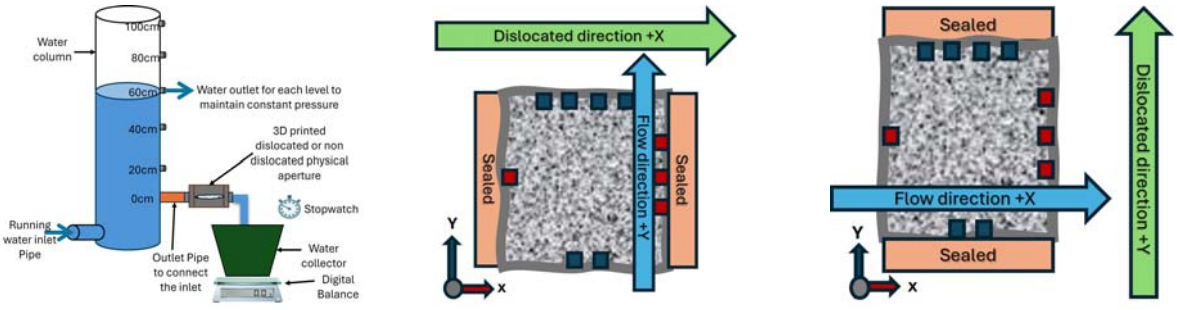
The fluid flow testing setup comprised a water column fitted with a custom-designed outlet pipe (Fig. 3b), which was connected to the inlet connector of the 3D-printed physical aperture model (Fig. 3a). The pipe system was designed to maintain uniform internal dimensions along the entire connection to ensure consistent flow conditions.



(a) (b)

Fig. 3(a) 3D-printed physical aperture model equipped with two connectors; (b) Outlet pipefitted to the water column.

A continuously running tap supplied the water column to ensure a steady and controlled flow of water. A constant pressure was maintained by varying the vertical distance between the water level at the model inlet and the water level in the column (Fig. 4a). For each experimental configuration, this height difference was adjusted in increments of 20 cm during the flow tests. At each 20 cm pressure step, the mass of water discharged from the outlet connector was collected over a fixed time period and measured using a digital balance with a precision of 0.1 g. The 3D-printed physical aperture models were used to conduct fluid flow experiments for different steps of dislocation, applied perpendicular to the flow direction, under varying pressure gradients. (Fig. 4b-c).



(a) (b) (c)

Fig. 4 (a) Schematic diagram of the fluid flow test apparatus and experimental setup; (b) Dislocation of the upper half of the specimen in the +X direction and fluid flow through the fracture in the +Y direction; (c) Dislocation of the upper half of the specimen in the +Y direction and fluid flow through the fracture in the +X direction.

3 Results and discussion

Fig. 5 shows the nonlinear relationship between volumetric flow rate (Q) and hydraulic pressure gradient (∇P) for the 3D-printed aperture models under both perfectly matched and displaced conditions. As anticipated, the flow rate increased with increasing pressure gradient. In addition, higher dislocation levels produced greater flow rates at the same pressure gradient. For further analysis, the data were fitted to the Forchheimer equation (Eq.1), and the hydraulic aperture (e_h) was calculated. These values were then compared with the corresponding physical apertures (e_m) of the rock specimen obtained in the previous study (Torkan et al. 2025). The results show that the hydraulic aperture increases with each increment of dislocation, consistent with the increase in physical aperture. This behaviour can be explained by the fact that increasing dislocation enlarges the physical aperture, which may also increase the hydraulic aperture, leading to enhanced fluid flow through the dislocated rough fracture. The results further indicate anisotropic flow behaviour, as both the measured flow rates and the derived hydraulic apertures depend on the magnitude of the dislocation and the flow direction (Fig. 5 and Fig. 6).

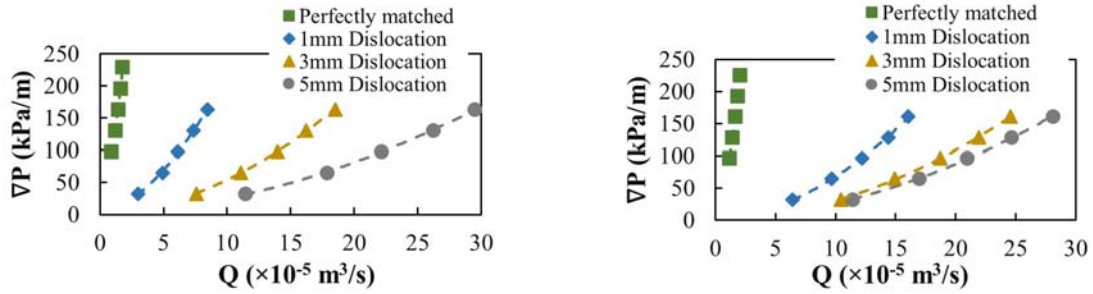


Fig. 5 Nonlinear relationship between flow rate and pressure gradient at dislocation levels:(a) Dislocation in the +X direction and fluid flow in the +Y direction; (b) Dislocation in the +Y direction and fluid flow in the +X direction.

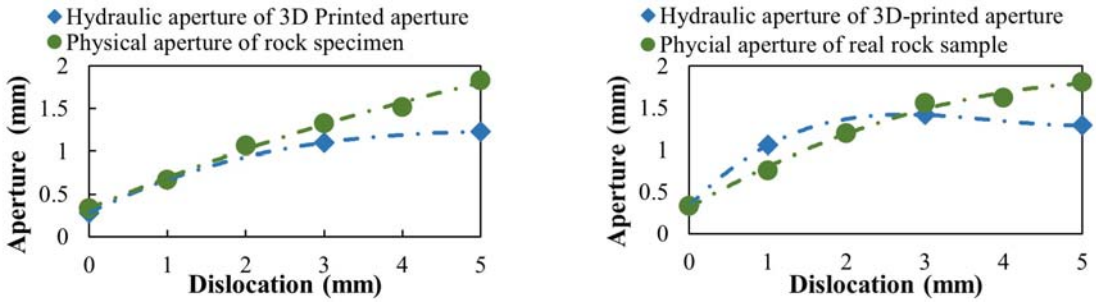


Fig. 6 Comparison between the physical apertures of the rock specimen and the hydraulic apertures of 3D printed apertures for various dislocation configurations:(a) Dislocation in the +X direction and fluid flow in the +Y direction; (b) Dislocation in the +Y direction and fluid flow in the +X direction.

The roughness of 3D-printed replicas may differ from that of real rock specimens due to constraints in 3D printing and photogrammetry. Fine-scale surface details of natural fractures may not be fully captured because of image resolution limits and processing constraints in photogrammetry. Similarly, in FDM 3D printing, additional loss of detail can occur due to the layer height and extrusion width. The resolution of printed surfaces can also vary in the horizontal and vertical directions depending on how the model is oriented on the build plate, while slicing tolerances may further influence the accuracy of the final geometry (Fig. 7b). Collectively, these factors generally result in smoother fracture surfaces compared to natural rock, which can lead to increased flow rates. In addition, introducing a uniform 0.4 mm gap between the fracture surfaces in the 3D-printed aperture may help improve replication accuracy, although the optimal gap size may vary depending on the degree of dislocation (Fig. 7a).

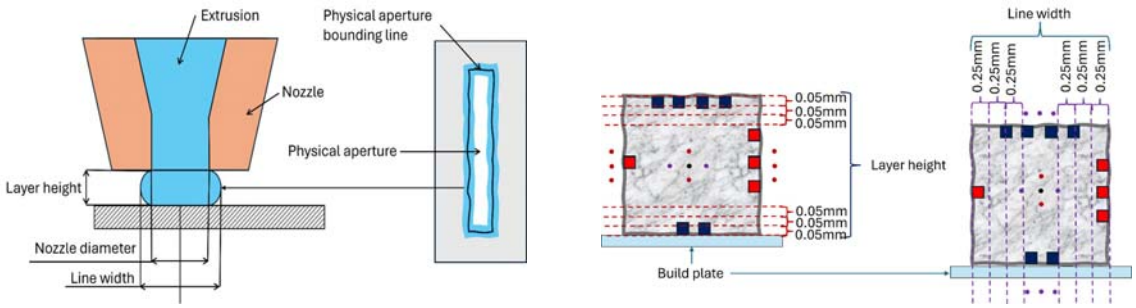


Fig. 7(a) Nozzle interference resulting in an undersized physical aperture; (b) Directional resolution variation in FDM 3D Printing: Influence of nozzle diameter and layer height (Liyanarathana Vidanage 2025).

4 Conclusion

A replica-based methodology integrating photogrammetry, 3D modelling, and FDM 3D printing was developed to investigate fluid flow behaviour in dislocated rock fractures under controlled and repeatable conditions. The experimental findings indicated that increasing fracture dislocation may lead to enlargement of both physical and hydraulic apertures, which in turn produces higher, nonlinear flow rates. Variations in flow behaviour further demonstrated anisotropic flow, influenced by both the extent and orientation of dislocation. Although limitations in photogrammetry and 3D printing resolution tend to smooth fine-scale fracture roughness, and the use of an optimal 0.4 mm gap may contribute to increased flow rates and hydraulic apertures in the replicas, the proposed framework remains effective for quantifying the impact of fracture dislocation on fluid flow. Overall, while photogrammetry-based reconstruction and 3D-printed models successfully reproduce key aperture characteristics and flow trends, challenges still exist in fully capturing the complexity of natural fracture geometries, especially under different dislocation conditions.

Acknowledgment

This work was a part of a master's thesis (Liyanarathana Vidanage 2025) at Aalto University and supported by the National Nuclear Safety and Waste Management Research Programme SAFER2028 (funding numbers SAFER 23/2025 MIRKAI, SAFER 32/2026 MIRKA II and DENSE). During the preparation of this work, the authors used ChatGPT to improve the language and readability. The authors reviewed and edited the content as needed and take full responsibility for the final publication.

References

Hakami E, Larsson E (1996) Aperture measurements and flow experiments on a single natural fracture. International Journal of Rock Mechanics and Mining Sciences & Geomechanics Abstracts 33(4):395-404. https://doi.org/10.1016/0148-9062(95)00070-4

Hakami E (1995) Aperture distribution of rock fractures. Doctoral thesis at Royal Institute of Technology.

Jiang C, Zhao GF (2015) A preliminary study of 3D printing on rock mechanics. Rock Mechanics and Rock Engineering 48(3): 1041–1050. https://doi.org/10.1007/s00603-014-0612-y

Liyanarathana Vidanage S (2025) Fluid flow tests for a non- and dislocated rock fracture of Kuru granite and its replicas. Master's thesis at Aalto University.

Torkan M, Janiszewski M, Uotinen L, Baghbanan A, Rinne M (2024) High-resolution photogrammetry to measure physical aperture of two separated rock fracture surfaces. Journal of Rock Mechanics and Geotechnical Engineering 16(8): 2922–2934. https://doi.org/10.1016/j.jrmge.2023.10.003

Torkan M, Liyanarathna Vidanage S, Aydogmus M, Uotinen L, Anttilainen A, Janiszewski M, Rinne M (2025) Measuring physical aperture of a fracture affected by dislocation using photogrammetry. ISRM International Symposium – EUROCK 2025, Trondheim, Norway.

Uotinen L, Torkan M, Janiszewski M, Baghbanan A, Nieminen V, Rinne M (2020) Characterization of hydro-mechanical properties of rock fractures using steady state flow tests. ISRM International Symposium – EUROCK 2020, Norsk Betongforening.

Zimmerman RW, Al-Yaarubi A, Pain CC, Grattoni CA (2004) Non-linear regimes of fluid flow in rock fractures. International Journal of Rock Mechanics and Mining Sciences 41(1): 163-169.https://doi.org/10.1016/j.ijrmms.2004.03.036